

Thermal quasi-particle theory

So Hirata*

Department of Chemistry, University of Illinois at Urbana-Champaign, Urbana, Illinois 61801, USA

(Dated: August 9, 2024)

The widely used thermal Hartree–Fock (HF) theory is generalized to include the effect of electron correlation while maintaining its quasi-independent-particle framework. An electron-correlated internal energy (or grand potential) is defined by the second-order finite-temperature many-body perturbation theory (MBPT), which then dictates the corresponding thermal orbital (quasi-particle) energies in such a way that all thermodynamic relations are obeyed. The associated density matrix is of the one-electron type, whose diagonal elements take the form of the Fermi–Dirac distribution functions, when the grand potential is minimized. The formulas for the entropy and chemical potential are unchanged from those of Fermi–Dirac or thermal HF theory. The theory thus postulates a finite-temperature extension of the second-order Dyson self-energy of one-particle many-body Green’s function theory and can be viewed as a second-order, diagonal, frequency-independent, thermal inverse Dyson equation. At low temperature, the theory approaches finite-temperature MBPT of the same order, but it outperforms the latter at intermediate temperature by including additional electron-correlation effects through orbital energies. A physical meaning of these thermal orbital energies (including that of thermal HF orbital energies, which has been elusive) is proposed.

I. INTRODUCTION

Thermal Hartree–Fock (HF) theory^{1–3} is a curious ansatz. It uses an auxiliary one-electron Hamiltonian to define its one-electron density matrix, whereas a true density matrix for thermodynamics governed by an interacting Hamiltonian should be much higher ranked.⁴ Its diagonal elements, as variational parameters, ultimately become the Fermi–Dirac distribution functions of the non-interacting Fermi–Dirac theory, when the grand potential is minimized. The state energies defining this grand potential are, however, evaluated with the exact Hamiltonian containing two-electron interactions. Stipulated in this way, the theory does not seem to correspond to a single, consistent grand partition function.

Nevertheless, the thermodynamic functions of this theory are shown^{3,5} to obey all thermodynamic relations. They also correctly reduce³ to the zero-temperature HF theory.^{6,7} They are widely used in applications to, e.g., energy bands in a solid where their temperature-dependent orbital energies are often invoked, somewhat unscrupulously, in explaining metal–insulator transitions,⁸ etc. This is in spite of the facts that their physical meaning is still obscure⁹ and that state energies in quantum mechanics are supposed to be constant of temperature.

In this article, inspired by the immense success of thermal HF theory, we generalize this ansatz to include the effects of electron correlation, while keeping to its quasi-independent-particle framework and grand canonical ensemble. Our strategy of postulating what we call *thermal quasi-particle theory* is as follows:

We first assume that every state consists of non-interacting quasi-particles, each occupying a well-defined orbital having an electron-correlated orbital energy in a Slater determinant. The internal energy (or equivalently, the grand potential) is postulated by consulting with finite-temperature many-body perturbation theory (MBPT).^{10–12} Its definition dictates the forms of the thermal quasi-particle energies (i.e., the electron-correlated thermal orbital energies) such that all thermodynamic relations are obeyed. The corresponding density matrix

is then of the one-electron type, whose diagonal elements take the form of the Fermi–Dirac distribution functions, when the grand potential is minimized. The formulas for the entropy and average number of electrons (determining the chemical potential) are unchanged from the corresponding formulas of Fermi–Dirac or thermal HF theory. The thermal quasi-particle energies thus defined are interpretable as a finite-temperature generalization^{13–16} of the Dyson self-energies of one-particle many-body Green’s function (MBGF) theory.¹⁷

Being based on perturbation theory, thermal quasi-particle theory forms a hierarchy of approximations with increasing accuracy and complexity. Fermi–Dirac and thermal HF theories can be viewed, respectively, as the zeroth- and first-order instances of this hierarchy. Here, we introduce a second-order thermal quasi-particle theory, which is the leading order in describing electron correlation, on the basis of the second-order grand potential or internal energy of finite-temperature MBPT.^{11,12} We propose the expression for the corresponding second-order thermal self-energies, which obey all thermodynamic relations and ensure the variationality of the grand potential. The theory thus constitutes a second-order, diagonal, frequency-independent, thermal inverse Dyson equation.¹⁷ It reduces to the second-order MBPT and MBGF (in the diagonal and frequency-independent approximation) at zero temperature.

A comparison of thermal quasi-particle theories with finite-temperature MBPT suggests that the former may include higher-order perturbation corrections through correlation-corrected thermal orbital energies and can thereby outperform the latter at intermediate temperatures. Furthermore, a comparison with thermal full-configuration-interaction (FCI) theory¹⁸ supports a proposed physical meaning of these thermal orbital energies, including that of thermal HF orbital energies, which has been elusive.^{9,12}

II. FERMI-DIRAC THEORY

Fermi-Dirac theory can be considered as the zeroth-order thermal quasi-particle theory [thermal QP(0) theory]. It is reviewed only briefly since it is discussed more fully in Ref. 3. Its internal energy $U^{(0)}$ and entropy $S^{(0)}$ at the inverse temperature $\beta = (k_B T)^{-1}$ are given by

$$U^{(0)} \equiv \langle E^{(0)} \rangle = \sum_p \epsilon_p^{(0)} f_p^-, \quad (1)$$

$$S^{(0)} \equiv -k_B (f_p^- \ln f_p^- + f_p^+ \ln f_p^+) \quad (2)$$

with the Fermi-Dirac distribution functions,

$$f_p^- = \frac{1}{1 + e^{\beta(\epsilon_p^{(0)} - \mu^{(0)})}}, \quad (3)$$

$$f_p^+ = 1 - f_p^- = \frac{e^{\beta(\epsilon_p^{(0)} - \mu^{(0)})}}{1 + e^{\beta(\epsilon_p^{(0)} - \mu^{(0)})}}. \quad (4)$$

Here, $\epsilon_p^{(0)}$ is the energy of the p th spinorbital of a reference wave function, and $\mu^{(0)}$ is the chemical potential determined by the electroneutrality condition,

$$\bar{N} = \sum_p f_p^-, \quad (5)$$

where \bar{N} is the average number of electrons, and the summations are always taken over all spinorbitals. The $\langle E^{(n)} \rangle$ in Eq. (1) is a zeroth-order thermal average of state energies, i.e.,

$$\langle E^{(n)} \rangle \equiv \frac{\sum_I E_I^{(n)} e^{-\beta(E_I^{(0)} - \mu^{(0)} N_I)}}{\sum_I e^{-\beta(E_I^{(0)} - \mu^{(0)} N_I)}}, \quad (6)$$

where $E_I^{(n)}$ is the n th-order perturbation correction to the energy of the I th Slater-determinant state according to Hirschfelder-Certain degenerate perturbation theory¹⁹ with $E_I^{(0)} = \sum_i \epsilon_i^{(0)}$ (i labels spinorbitals occupied in the I th state). Sum-over-states expressions of the thermal averages can be reduced to sum-over-orbital ones either by combinatorial logic^{10,11} or by normal-ordered second quantization at finite temperature.¹²

The grand potential $\Omega^{(0)}$ is then given by

$$\Omega^{(0)} \equiv U^{(0)} - \mu^{(0)} \bar{N} - TS^{(0)} \quad (7)$$

$$= \sum_p (\epsilon_p^{(0)} - \mu^{(0)}) f_p^- + \frac{1}{\beta} \sum_p (f_p^- \ln f_p^- + f_p^+ \ln f_p^+). \quad (8)$$

As explicitly shown in Ref. 3, they satisfy the thermodynamic relations such as Eq. (7) and

$$-\frac{\partial \Omega^{(0)}}{\partial \mu^{(0)}} = \bar{N}, \quad (9)$$

$$-\frac{\partial \Omega^{(0)}}{\partial T} = S^{(0)}. \quad (10)$$

The Fermi-Dirac distribution function [Eq. (3)] is a diagonal element of the one-electron density matrix that minimizes the grand potential. Therefore,

$$\frac{\partial \Omega^{(0)}}{\partial f_p^-} = 0, \quad (11)$$

which is also easily verifiable.³

Fermi-Dirac theory is an exact theory for thermodynamics of a system governed by an independent-particle Hamiltonian.

III. THERMAL HARTREE-FOCK THEORY

Thermal HF theory^{1,2} is the first-order instance of thermal quasi-particle theory [thermal QP(1) theory], which is also fully discussed in Ref. 3. It accommodates the exact Hamiltonian with two-electron interactions within a quasi-independent-particle framework. Its internal energy U^{HF} is postulated by an intuitively natural finite-temperature generalization of the zero-temperature HF energy,¹² i.e.,

$$U^{\text{HF}} \equiv \langle E^{(0)} \rangle + \langle E^{(1)} \rangle \quad (12)$$

$$= \sum_p \epsilon_p^{\text{HF}} f_p^- - \frac{1}{2} \sum_{p,q} \langle pq || pq \rangle f_p^- f_q^- \quad (13)$$

with

$$\epsilon_p^{\text{HF}} \equiv h_{pp} + \sum_r \langle pr || pr \rangle f_r^-, \quad (14)$$

where h_{pq} is the one-electron (“core”) part of the Hamiltonian matrix element,⁶ $\langle pq || rs \rangle$ is an anti-symmetrized two-electron integral,^{6,7} and $\langle E^{(1)} \rangle$ has been reduced in Eqs. (45) and (46) of Ref. 11. Spinorbitals labeled by p and q are the ones that bring the matrix of thermal HF orbital energies ϵ^{HF} into a diagonal form, i.e.,

$$\epsilon_{pq}^{\text{HF}} = h_{pq} + \sum_r \langle pr || qr \rangle f_r^- = \begin{cases} \epsilon_p^{\text{HF}} & (p = q); \\ 0 & (p \neq q), \end{cases} \quad (15)$$

The Fermi-Dirac distribution functions,

$$f_p^- = \frac{1}{1 + e^{\beta(\epsilon_p^{\text{HF}} - \mu^{\text{HF}})}}, \quad (16)$$

$$f_p^+ = 1 - f_p^- = \frac{e^{\beta(\epsilon_p^{\text{HF}} - \mu^{\text{HF}})}}{1 + e^{\beta(\epsilon_p^{\text{HF}} - \mu^{\text{HF}})}}, \quad (17)$$

are now defined with ϵ_p^{HF} and μ^{HF} . The latter is determined by the same electroneutrality condition,

$$\bar{N} = \sum_p f_p^-. \quad (18)$$

The entropy formula is unchanged from that of Fermi-Dirac theory [Eq. (2)],

$$S^{\text{HF}} \equiv -k_B \sum_p (f_p^- \ln f_p^- + f_p^+ \ln f_p^+). \quad (19)$$

The grand potential is therefore given by

$$\Omega^{\text{HF}} \equiv U^{\text{HF}} - \mu^{\text{HF}} \bar{N} - TS^{\text{HF}} \quad (20)$$

$$= \sum_p (\epsilon_p^{\text{HF}} - \mu^{\text{HF}}) f_p^- - \frac{1}{2} \sum_{p,q} \langle pq || pq \rangle f_p^- f_q^- + \frac{1}{\beta} \sum_p (f_p^- \ln f_p^- + f_p^+ \ln f_p^+). \quad (21)$$

These thermodynamic functions together satisfy³ the thermodynamic relations such as Eq. (20) by construction as well as

$$-\frac{\partial \Omega^{\text{HF}}}{\partial \mu^{\text{HF}}} = \bar{N}, \quad (22)$$

$$-\frac{\partial \Omega^{\text{HF}}}{\partial T} = S^{\text{HF}}, \quad (23)$$

$$\frac{\partial \Omega^{\text{HF}}}{\partial f_p^-} = 0. \quad (24)$$

The last identity proves that Ω^{HF} is indeed minimized^{2,3} by the orbitals that diagonalize ϵ^{HF} [Eq. (15)] and by the one-particle density matrix whose eigenvalues are the Fermi–Dirac distribution functions of Eq. (16).

IV. THERMAL QUASI-PARTICLE THEORY

Second-order thermal quasi-particle theory [thermal QP(2) theory] is postulated by its internal energy,

$$U^{\text{QP}(2)} \equiv \langle E^{(0)} \rangle + \langle E^{(1)} \rangle + \langle E^{(2)} \rangle. \quad (25)$$

The last term $\langle E^{(2)} \rangle$ is the thermal average of second-order (degenerate) perturbation energies¹⁹ and has been reduced in Eqs. (C7) and (C8) of Ref. 11 to the following sum-over-orbitals formula:

$$\langle E^{(2)} \rangle = \sum_{p,q}^{\text{denom.} \neq 0} \frac{F_{qp} F_{pq}}{\epsilon_p^{(0)} - \epsilon_q^{(0)}} f_p^- f_q^+ + \frac{1}{4} \sum_{p,q,r,s}^{\text{denom.} \neq 0} \frac{\langle pq || rs \rangle \langle rs || pq \rangle}{\epsilon_p^{(0)} + \epsilon_q^{(0)} - \epsilon_r^{(0)} - \epsilon_s^{(0)}} f_p^- f_q^- f_r^+ f_s^+. \quad (26)$$

with

$$F_{pq} \equiv \epsilon_{pq}^{\text{HF}} - \delta_{pq} \epsilon_p^{(0)}, \quad (27)$$

where “denom. $\neq 0$ ” restricts the summation to over those indexes whose denominator is nonzero.^{11,12}

It is a natural finite-temperature generalization of second-order many-body perturbation energy,^{7,20} but is considerably simpler than the full second-order correction to the internal energy $U^{(2)}$ of finite-temperature MBPT [Eq. (74) of Ref. 11]. The simplification is at least partly justified by the equally simpler treatments of the chemical-potential and entropy contributions to adhere to the quasi-independent-particle framework that the theory adopts. The first term of $\langle E^{(2)} \rangle$ [Eq. (26)]

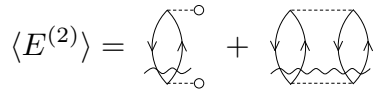


FIG. 1. Shavitt–Bartlett-style diagrams^{7,12} of $\langle E^{(2)} \rangle$ of Eq. (26). Each downgoing (upgoing) edge represents f_p^- (f_p^+), a dashed line is an anti-symmetrized two-electron integral, a dashed line with a circle denotes F_{pq} , and a wiggly (resolvent) line is a denominator factor.

is the so-called non-HF term (or more precisely, non-thermal-HF term, in this case),⁷ which is zero when thermal HF theory is used as the reference (where $F_{pq} = 0$). The diagrammatic representation¹² of $\langle E^{(2)} \rangle$ is given in Fig. 1.

We thus have

$$\begin{aligned} U^{\text{QP}(2)} \equiv & \sum_p \epsilon_p^{\text{HF}} f_p^- - \frac{1}{2} \sum_{p,q} \langle pq || pq \rangle f_p^- f_q^- \\ & + \sum_{p,q}^{\text{denom.} \neq 0} \frac{F_{qp} F_{pq}}{\epsilon_p^{(0)} - \epsilon_q^{(0)}} f_p^- f_q^+ \\ & + \frac{1}{4} \sum_{p,q,r,s}^{\text{denom.} \neq 0} \frac{\langle pq || rs \rangle \langle rs || pq \rangle}{\epsilon_p^{(0)} + \epsilon_q^{(0)} - \epsilon_r^{(0)} - \epsilon_s^{(0)}} f_p^- f_q^- f_r^+ f_s^+. \end{aligned} \quad (28)$$

The entropy formula retains the one-particle picture and takes the form,

$$S^{\text{QP}(2)} \equiv -k_B \sum_p (f_p^- \ln f_p^- + f_p^+ \ln f_p^+), \quad (29)$$

which differs materially from the $S^{(0)} + S^{(1)} + S^{(2)}$ of Refs. 11 and 12, but is more in line with thermal HF or Fermi–Dirac theory. The corresponding grand potential is then defined by

$$\begin{aligned} \Omega^{\text{QP}(2)} \equiv & U^{\text{QP}(2)} - \mu^{\text{QP}(2)} \bar{N} - TS^{\text{QP}(2)} \\ = & \sum_p (\epsilon_p^{\text{HF}} - \mu^{\text{QP}(2)}) f_p^- - \frac{1}{2} \sum_{p,q} \langle pq || pq \rangle f_p^- f_q^- \\ & + \frac{1}{\beta} \sum_p (f_p^- \ln f_p^- + f_p^+ \ln f_p^+) + \langle E^{(2)} \rangle, \end{aligned} \quad (31)$$

where $\mu^{\text{QP}(2)}$ is the chemical potential, which is determined by the same electroneutrality condition of Fermi–Dirac theory, i.e.,

$$\bar{N} = \sum_p f_p^-. \quad (32)$$

Spinorbitals labeled by p and q are those of a reference theory, which is typically but not limited to zero-temperature HF theory or thermal HF theory at the same T . No orbital rotation by matrix diagonalization is performed in this ansatz, but $\Omega^{\text{QP}(2)}$ is still minimized with respect to the diagonal elements of the one-electron density matrix, which are none other than the f_p^- .

These f_p^\mp take the form of the Fermi–Dirac distribution functions, when $\Omega^{\text{QP}(2)}$ is minimized by varying f_p^- (see below

for a proof).³ They are defined with the second-order quasi-particle energy $\epsilon_p^{\text{QP}(2)}$ and chemical potential $\mu^{\text{QP}(2)}$, i.e.,

$$f_p^- = \frac{1}{1 + e^{\beta(\epsilon_p^{\text{QP}(2)} - \mu^{\text{QP}(2)})}}, \quad (33)$$

$$f_p^+ = 1 - f_p^- = \frac{e^{\beta(\epsilon_p^{\text{QP}(2)} - \mu^{\text{QP}(2)})}}{1 + e^{\beta(\epsilon_p^{\text{QP}(2)} - \mu^{\text{QP}(2)})}} \quad (34)$$

with $\epsilon_p^{\text{QP}(2)}$ given by

$$\epsilon_p^{\text{QP}(2)} = \epsilon_p^{\text{HF}} + \Sigma_{pp}^{(2)}. \quad (35)$$

Here, $\Sigma_{pp}^{(2)}$ is a finite-temperature analogue of the second-order self-energy of MBGF.¹⁷ In a zero-temperature reference, where $\epsilon_p^{(0)}$ is constant of T , it takes the form of

$$\begin{aligned} \Sigma_{pp}^{(2)} = & \sum_q^{\text{denom.} \neq 0} \frac{F_{qp} F_{pq}}{\epsilon_p^{(0)} - \epsilon_q^{(0)}} f_q^+ - \sum_q^{\text{denom.} \neq 0} \frac{F_{qp} F_{pq}}{\epsilon_q^{(0)} - \epsilon_p^{(0)}} f_q^- \\ & + \sum_{q,r}^{\text{denom.} \neq 0} \frac{\langle qr || pr \rangle F_{pq}}{\epsilon_p^{(0)} - \epsilon_q^{(0)}} f_p^- f_q^+ \\ & + \sum_{q,r}^{\text{denom.} \neq 0} \frac{F_{qp} \langle pr || qr \rangle}{\epsilon_p^{(0)} - \epsilon_q^{(0)}} f_p^- f_q^+ \\ & + \frac{1}{2} \sum_{q,r,s}^{\text{denom.} \neq 0} \frac{\langle pq || rs \rangle \langle rs || pq \rangle}{\epsilon_p^{(0)} + \epsilon_q^{(0)} - \epsilon_r^{(0)} - \epsilon_s^{(0)}} f_q^- f_r^+ f_s^+ \\ & - \frac{1}{2} \sum_{q,r,s}^{\text{denom.} \neq 0} \frac{\langle rs || pq \rangle \langle pq || rs \rangle}{\epsilon_r^{(0)} + \epsilon_s^{(0)} - \epsilon_p^{(0)} - \epsilon_q^{(0)}} f_q^+ f_r^- f_s^-, \quad (36) \end{aligned}$$

which is obtained by demanding all thermodynamic relations be obeyed by thermodynamic functions defined by this theory (see below for a derivation). A diagrammatic representation of $\Sigma_{pp}^{(2)}$ is given in Fig. 2.

The first two terms of the above equation (or the first two diagrams in Fig. 2) are the so-called semi-reducible diagrams of $\Delta\text{MP}2$.²¹ Not only do they account for the non-HF-reference contributions,⁷ but they correct the errors arising from the diagonal approximation to the self-energy implicit in the $\Delta\text{MP}n$ ansatz.²¹ Thanks to these diagrams, which are illegal in the Feynman–Dyson perturbation expansion of MBGF,¹⁷ $\Delta\text{MP}n$ is convergent at the exactness (and, in fact, more reliably so²² than Feynman–Dyson MBGF) while using the diagonal and frequency-independent approximations throughout the perturbation orders. In this sense, the thermal self-energy thus defined may be a finite-temperature analogue of $\Delta\text{MP}n$ than of Feynman–Dyson MBGF.

The third and fourth terms (diagrams) are non-HF terms⁷ and are also related to the energy-independent diagrams.^{23,24}

When a zero-temperature HF reference is used, in the $T = 0$ limit, the first four terms vanish because $F_{pq} = 0$, leaving only the last two terms as the zero-temperature second-order self-energy in the diagonal, frequency-independent approximation. Their diagrams (the last two in Fig. 2) are, therefore, isomorphic to the two second-order self-energy diagrams

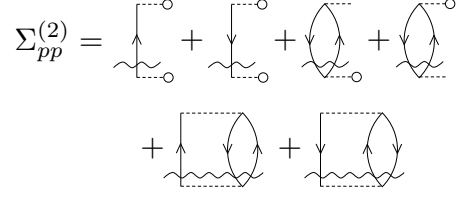


FIG. 2. Second-order thermal Dyson self-energy diagrams in the zero-temperature reference [Eq. (36)], which are obtained by cutting an edge in each of the internal energy diagrams in Fig. 1 and trimming the dangling lines. See also the caption of Fig. 1 as well as Refs. 12 and 17.

(e.g., Fig. 4 of Ref. 17), although their scope is different (the former are for $T \geq 0$, while the latter are only for $T = 0$).

With these definitions, the thermodynamic relation of Eq. (30) is satisfied by construction. The next one,

$$-\frac{\partial \Omega^{\text{QP}(2)}}{\partial \mu^{\text{QP}(2)}} = \bar{N}, \quad (37)$$

is also obeyed, which can be confirmed by explicit evaluation of the derivative.

$$\begin{aligned} -\frac{\partial \Omega^{\text{QP}(2)}}{\partial \mu^{\text{QP}(2)}} = & -\sum_p \frac{\partial \epsilon_p^{\text{HF}}}{\partial \mu^{\text{QP}(2)}} f_p^- + \sum_p f_p^- \\ & - \sum_p (\epsilon_p^{\text{HF}} - \mu^{\text{QP}(2)}) \frac{\partial f_p^-}{\partial \mu^{\text{QP}(2)}} \\ & + \sum_{p,q} \langle pq || pq \rangle \frac{\partial f_p^-}{\partial \mu^{\text{QP}(2)}} f_q^- \\ & - \frac{1}{\beta} \sum_p \frac{\partial f_p^-}{\partial \mu^{\text{QP}(2)}} \ln f_p^- - \frac{1}{\beta} \sum_p \frac{\partial f_p^-}{\partial \mu^{\text{QP}(2)}} \\ & - \frac{1}{\beta} \sum_p \frac{\partial f_p^+}{\partial \mu^{\text{QP}(2)}} \ln f_p^+ - \frac{1}{\beta} \sum_p \frac{\partial f_p^+}{\partial \mu^{\text{QP}(2)}} - \frac{\partial \langle E^{(2)} \rangle}{\partial \mu^{\text{QP}(2)}} \\ = & \sum_p f_p^- - \sum_p (\epsilon_p^{\text{HF}} - \mu^{\text{QP}(2)}) \frac{\partial f_p^-}{\partial \mu^{\text{QP}(2)}} \\ & - \frac{1}{\beta} \sum_p \frac{\partial f_p^-}{\partial \mu^{\text{QP}(2)}} \ln \frac{f_p^-}{f_p^+} - \frac{\partial \langle E^{(2)} \rangle}{\partial \mu^{\text{QP}(2)}} \\ = & \sum_p f_p^- + \sum_p \Sigma_{pp}^{(2)} \frac{\partial f_p^-}{\partial \mu^{\text{QP}(2)}} - \frac{\partial \langle E^{(2)} \rangle}{\partial \mu^{\text{QP}(2)}} \\ = & \sum_p f_p^- = \bar{N}, \quad (38) \end{aligned}$$

where we used

$$\frac{\partial f_p^+}{\partial \mu^{\text{QP}(2)}} = -\frac{\partial f_p^-}{\partial \mu^{\text{QP}(2)}}, \quad (39)$$

$$\ln \frac{f_p^-}{f_p^+} = -\beta (\epsilon_p^{\text{QP}(2)} - \mu^{\text{QP}(2)}), \quad (40)$$

but not the explicit derivative $\partial f_p^- / \partial \mu^{\text{QP}(2)}$, which is a solution of a system of linear equations and cannot be written in a closed form.³ This justifies Eq. (32).

In the penultimate equality of Eq. (38), we also used

$$\sum_p \Sigma_{pp}^{(2)} \frac{\partial f_p^-}{\partial \mu^{\text{QP}(2)}} = \frac{\partial \langle E^{(2)} \rangle}{\partial \mu^{\text{QP}(2)}}, \quad (41)$$

which can be verified by using Eqs. (26) and (36). In fact, the form of $\Sigma_{pp}^{(2)}$ is determined in the first place from the general condition,

$$\Sigma_{pp}^{(n)} \equiv \frac{\partial \langle E^{(n)} \rangle}{\partial f_p^-}, \quad (42)$$

which ensures that Eq. (41) and all similar relations be satisfied. The $\Sigma_{pp}^{(2)}$ formula of Eq. (36) was postulated by substituting Eq. (26) into the above formula.

Equation (42) is a finite-temperature generalization^{13,14} of the n th-order self-energy of MBGF,^{17,21} which is diagonal and frequency independent. Owing to the diagonal construction, the second- and higher-order thermal quasi-particle theory does not involve rotation of orbitals, unlike thermal HF theory^{2,3} or Feynman–Dyson MBGF,¹⁷ which define the HF or Dyson orbitals²⁵ as those that bring the Fock or self-energy matrix into a diagonal form. Despite the absence of orbital rotation, $\Omega^{\text{QP}(2)}$ is still minimized by varying f_p^- (see below).

Diagrammatically, the differentiation with respect to f_p^- corresponds to opening a closed, internal-energy diagram by deleting an edge.¹⁷ A possible physical meaning of thermal self-energies or thermal quasi-particle energies, which are temperature dependent, is given and discussed in Sec. VI.

The following thermodynamic relation,

$$-\frac{\partial \Omega^{\text{QP}(2)}}{\partial T} = S^{\text{QP}(2)}, \quad (43)$$

is also obeyed. This too can be confirmed by explicit differentiation.

$$\begin{aligned} -\frac{\partial \Omega^{\text{QP}(2)}}{\partial T} &= k_B \beta^2 \frac{\partial \Omega^{\text{QP}(2)}}{\partial \beta} \\ &= k_B \beta^2 \sum_p \frac{\partial \epsilon_p^{\text{HF}}}{\partial \beta} f_p^- \\ &\quad + k_B \beta^2 \sum_p (\epsilon_p^{\text{HF}} - \mu^{\text{QP}(2)}) \frac{\partial f_p^-}{\partial \beta} \\ &\quad - k_B \beta^2 \sum_{p,q} \langle pq||pq \rangle \frac{\partial f_p^-}{\partial \beta} f_q^- \\ &\quad - k_B (f_p^- \ln f_p^- + f_p^+ \ln f_p^+) \\ &\quad + k_B \beta \sum_p \frac{\partial f_p^-}{\partial \beta} \ln \frac{f_p^-}{f_p^+} \\ &\quad + k_B \beta^2 \frac{\partial \langle E^{(2)} \rangle}{\partial \beta} \\ &= -k_B (f_p^- \ln f_p^- + f_p^+ \ln f_p^+) \\ &\quad - k_B \beta^2 \sum_p \frac{\partial \Sigma_{pp}^{(2)}}{\partial \beta} f_p^- + k_B \beta^2 \frac{\partial \langle E^{(2)} \rangle}{\partial \beta} \\ &= -k_B (f_p^- \ln f_p^- + f_p^+ \ln f_p^+) = S^{\text{QP}(2)}, \quad (44) \end{aligned}$$

where we used Eqs. (40) and (42), but not the explicit derivative $\partial f_p^- / \partial \beta$.³ This justifies Eq. (29).

It can also be shown that thermal QP(2) theory is variational with respect to the diagonal elements of its one-electron density matrix, but not with respect to orbitals.

$$\begin{aligned} \frac{\partial \Omega^{\text{QP}(2)}}{\partial f_p^-} &= (\epsilon_p^{\text{HF}} - \mu^{\text{QP}(2)}) + \frac{1}{\beta} \ln \frac{f_p^-}{f_p^+} + \frac{\partial \langle E^{(2)} \rangle}{\partial f_p^-} \\ &= (\epsilon_p^{\text{HF}} - \mu^{\text{QP}(2)}) - (\epsilon_p^{\text{QP}(2)} - \mu^{\text{QP}(2)}) + \Sigma_{pp}^{(2)} = 0, \end{aligned} \quad (45)$$

where Eq. (42) was used. This proves that the f_p^- functions that minimize $\Omega^{\text{QP}(2)}$ take the forms of the Fermi–Dirac distribution functions, justifying Eqs. (33) and (34).

Insofar as Eq. (42) is satisfied (and thus all thermodynamic relations are obeyed and the variationality is ensured), there is considerable latitude in selecting the functional form of an approximate internal energy. For instance, the most notable departure of $U^{\text{QP}(2)}$ in Eq. (28) from the lengthy, but full $U^{(2)}$ of Eq. (74) of Ref. 11 is the absence of the so-called anomalous-diagram terms,^{14,26} which sum over the set of indexes whose fictitious denominator is zero.^{11,12} They are purposefully neglected in our ansatz because they are found to cause a severe Kohn–Luttinger nonconvergence problem in $\Sigma_{pp}^{(2)}$,^{14,26–28} and are undesirable from both theoretical and practical points of view. This issue will be expounded in Appendix A.

When the reference wave function is supplied by a finite-temperature theory, its $\epsilon_p^{(0)}$ depends on temperature and the formulas for the thermal self-energies need to be adjusted accordingly. In the thermal HF reference, the *second-order* thermal self-energy $\Sigma_{pp}^{(2)}$ is found to contain *third-order* energy-independent diagrams^{23,24} among others (not considered further in this study).

Not only does finite-temperature MBPT suffer from the aforementioned Kohn–Luttinger nonconvergence,^{27,28} but the Feynman–Dyson perturbation series of zero-temperature MBGF is also shown to display even severer divergence for most low- and high-lying states.²² The impact of the latter divergence on thermal quasi-particle theories will be touched upon in Appendix B.

V. THERMODYNAMIC FUNCTIONS

Tables I–IV list the thermodynamic functions (Ω , U , μ , and S) of thermal HF [thermal QP(1)],³ thermal QP(2), finite-temperature MBPT(2),^{11,12} and thermal FCI theories¹⁸ for an ideal gas of the identical hydrogen fluoride molecules in a wide range of temperature (T). Figures 3–6 plot the deviations from thermal FCI benchmarks, the latter being exact within a basis set. The thermal QP(2) and finite-temperature MBPT(2) calculations were based on the zero-temperature HF reference. See Ref. 3 for the data for the same system from Fermi–Dirac [thermal QP(0)] theory and other thermal mean-field theories.

In all cases, thermal QP(2) results are close to finite-temperature MBPT(2) ones at low T and are more accurate

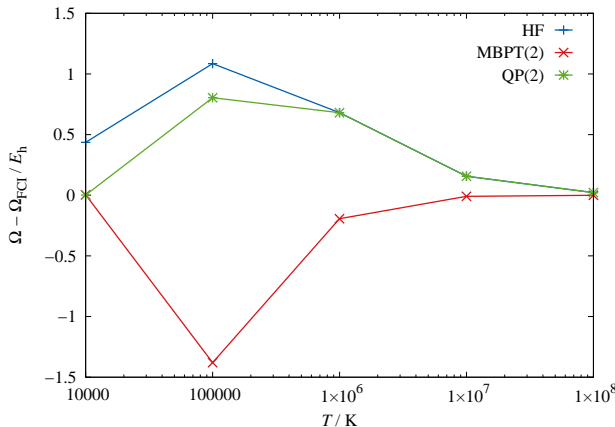


FIG. 3. The deviation from thermal FCI theory in grand potential Ω of the hydrogen fluoride molecule (0.9168 Å) in the STO-3G basis set as a function of temperature. The “HF” stands for thermal HF theory [thermal QP(1) theory], “MBPT(2)” denotes the second-order finite-temperature many-body perturbation theory with the zero-temperature HF reference, “QP(2)” designates the second-order thermal quasi-particle theory with the zero-temperature HF reference.

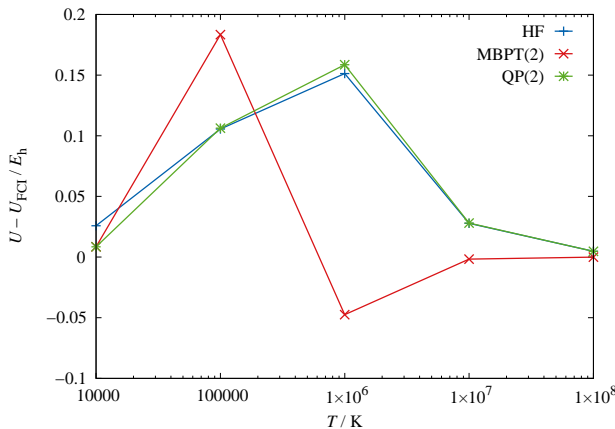


FIG. 4. Same as Fig. 3 but for internal energy U .

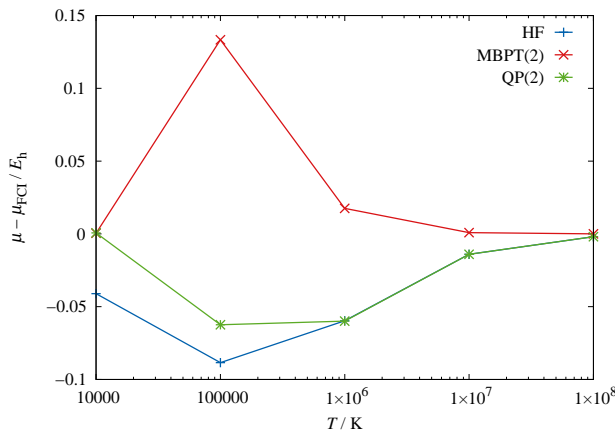


FIG. 5. Same as Fig. 3 but for chemical potential μ .

TABLE I. Grand potential Ω (in E_h) of the hydrogen fluoride molecule (0.9168 Å) in the STO-3G basis set as a function of temperature (T).

T / K	QP(1)=HF ^a	MBPT(2) ^b	QP(2) ^c	FCI ^d
10^4	-99.50758	-99.94001	-99.94179	-99.94377
10^5	-101.02137	-103.48646	-101.30273	-102.10659
10^6	-150.56294	-151.43748	-150.56368	-151.24440
10^7	-729.93806	-730.10421	-729.93862	-730.09519
10^8	-6846.98049	-6847.00261	-6846.98055	-6847.00247

^a First-order thermal quasi-particle theory or thermal HF theory.

^b Second-order finite-temperature MBPT^{10–12} with zero-temperature HF reference.

^c Second-order thermal quasi-particle theory with zero-temperature HF reference.

^d Thermal FCI theory.¹⁸

TABLE II. Same as Table I but for internal energy U (in E_h).

T / K	QP(1)=HF ^a	MBPT(2) ^b	QP(2) ^c	FCI ^d
10^4	-98.57076	-98.58809	-98.58810	-98.59658
10^5	-97.94385	-97.86604	-97.94314	-98.04938
10^6	-96.79410	-96.99284	-96.78681	-96.94534
10^7	-92.02773	-92.05724	-92.02752	-92.05557
10^8	-88.48266	-88.48744	-88.48268	-88.48740

^a–^d See the corresponding footnotes of Table I.

than thermal HF theory. This is expected because both thermal QP(2) theory and finite-temperature MBPT(2) reduce to zero-temperature MBPT(2), accounting for electron correlation, while thermal HF theory and its zero-temperature counterpart do not. At higher T , thermal QP(2) theory quickly approaches thermal HF theory, where their quasi-independent-particle picture becomes relatively less erroneous. However, at $T = 10^6$ K and 10^7 K, finite-temperature MBPT(2) is systematically more accurate as it accounts for the effect of electron correlation in S and μ and it uses more complete second-order corrections (including anomalous-diagram terms) in Ω and U . At the intermediate temperature of $T = 10^5$ K, thermal QP(2) theory (or even thermal HF theory) outperforms finite-temperature MBPT(2). This may be ascribed to the fact that thermal QP(2) theory includes the effect of electron correlation in the orbital energies, and thus higher-order correlation corrections in a manner similar in spirit to self-consistent Green’s function methods,^{14,16,29–40} which are said to work for strong correlation. However, this similarity must not be

TABLE III. Same as Table I but for chemical potential μ (in E_h).

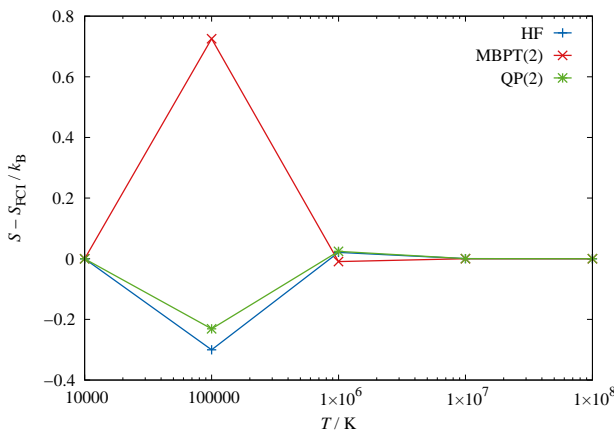
T / K	QP(1)=HF ^a	MBPT(2) ^b	QP(2) ^c	FCI ^d
10^4	0.09368	0.13519	0.13537	0.13472
10^5	0.20722	0.42903	0.23324	0.29568
10^6	3.80022	3.87744	3.79999	3.85990
10^7	46.85490	46.86975	46.85489	46.86892
10^8	504.65280	504.65478	504.65280	504.65476

^a–^d See the corresponding footnotes of Table I.

TABLE IV. Same as Table I but for entropy S (in k_B).

T / K	QP(1)=HF ^a	MBPT(2) ^b	QP(2) ^c	FCI ^d
10^4	0.00000	0.00001	0.00001	0.00011
10^5	3.17451	4.20017	3.24367	3.47472
10^6	4.97871	4.94828	4.98197	4.95769
10^7	5.34800	5.34763	5.34803	5.34766
10^8	5.40597	5.40596	5.40597	5.40596

^{a-d} See the corresponding footnotes of Table I.

FIG. 6. Same as Fig. 3 but for entropy S .

overstated because self-consistent Green's function methods replace reference orbitals and orbital energies by electron-correlated counterparts, while thermal QP(2) theory uses correlated orbital energies only in the Fermi-Dirac distribution functions and thus reduces identically to MBPT(2) at $T = 0$.

VI. THERMAL QUASI-PARTICLE ENERGIES

Equation (42) can be rewritten as

$$\epsilon_p \equiv \frac{\partial U}{\partial f_p}, \quad (46)$$

encompassing Fermi-Dirac, thermal HF, and thermal QP(2) theories.

The ϵ_p has the literal physical meaning of the increase in the internal energy upon infusion of an infinitesimal fraction of an electron in the p th spinorbital. While it is not irrational to speak about a fraction of an electron here because the process in question is the thermal average of the same processes involving an infinite number of particles, it is unclear how this quantity can be used in relation to observables.

The ϵ_p at $T = 0$ is rigorously connected with an ionization or electron-attachment energy via Koopmans' theorem⁶ or MBGF.¹⁷ However, such an interpretation will face difficulty when $T \gg 0$ because ionization or electron attachment at finite temperature will involve different orbitals at different probabilities, even in a strict independent-particle picture.

Just for convenience of the following analysis, let us define the internal energy $U(N)$ as a function of the average number of electrons N (which may now differ from \bar{N}) by the respective formula of U with only the chemical potential adjusted. For instance, the internal energy of thermal FCI theory is given by

$$U^{\text{FCI}}(N) = \frac{\sum_I E_I^{\text{FCI}} e^{-\beta(E_I^{\text{FCI}} - \mu N_I)}}{\sum_I e^{-\beta(E_I^{\text{FCI}} - \mu N_I)}}, \quad (47)$$

in which only the μ is adjusted for a given N to satisfy,

$$N = \frac{\sum_I N_I e^{-\beta(E_I^{\text{FCI}} - \mu N_I)}}{\sum_I e^{-\beta(E_I^{\text{FCI}} - \mu N_I)}}. \quad (48)$$

This is a valid and in fact, exact (within a basis set) treatment of thermodynamics if the particles are not electrically charged. For electrons, however, it describes a physically unrealistic, massively charged plasma, whose energy is not even extensive.⁴¹⁻⁴³ Nevertheless, $U(N)$ is computationally well defined even for electrons thanks to the ideal-gas assumption (i.e., no interactions between molecules) and will be useful for the following analysis.

For Fermi-Dirac, thermal HF, and thermal QP(2) theories, the internal energy $U(N)$ as a function of N is defined by Eqs. (1), (13), and (28), respectively, with its μ determined for a given N by

$$N = \sum_p f_p^-, \quad (49)$$

which no longer stands for electroneutrality. Then, $U(N-1) - U(N)$ may be considered as a crude estimate of the thermal average of the first ionization energies. Likewise, $U(N) - U(N+1)$ is an approximate thermal first electron-attachment energy. At $T = 0$, they correspond to the energy (the sign reversed) of the highest-occupied and lowest-unoccupied molecular or Dyson²⁵ orbitals (HOMO and LUMO), respectively, according to Koopmans' theorem⁶ or MBGF.¹⁷ Since $U(N)$ is defined and computed with ϵ_p , these internal-energy differences may furnish a physical meaning of the latter, which is indirect, yet potentially useful in relation to observables.

We call $U(N) - U(N-1)$ the thermal ionization energy and $U(N+1) - U(N)$ the thermal electron-attachment energy. Note the uncommon sign convention.

The $U(N)$ thus defined are computed for an ideal gas of identical hydrogen fluoride molecules by thermal FCI, thermal QP(2), and thermal HF theories in Figs. 7, 8, and 9, respectively. The thermal ionization energies $U(N) - U(N-1)$ of these three methods are compared with one another and also with the thermal HOMO energies in Table V. The same data for electron-attachment energies and LUMO are compiled in Table VI.

From the tables, we observe that while the HOMO and LUMO energies of thermal quasi-particle theories correctly reduce to the ionization and electron-attachment energies of MBGF in the $T = 0$ limit, they clearly have nothing to do with the approximate ionization or electron-attachment energies (as defined by $U(N) - U(N-1)$ or $U(N+1) - U(N)$ of

TABLE V. Thermal ionization energy (in E_h) of the hydrogen fluoride molecule (0.9168 Å) in the STO-3G basis set as a function of temperature (T).

T / K	Thermal HOMO energy		$U(N) - U(N - 1)$		
	QP(1)=HF ^a	QP(2) ^b	QP(1)=HF ^a	QP(2) ^b	FCI ^c
0 ^d	-0.46417	-0.39557	-0.46417	-0.39557	-0.40429
10^4	-0.46417	-0.39557	-0.46589	-0.39603	-0.40468
10^5	-0.45147	-0.46765	-0.21004	-0.18425	-0.32041
10^6	-0.57384	-0.58577	-0.57181	-0.57425	-0.77028
10^7	-0.69361	-0.69692	-3.40146	-3.40165	-3.65153
10^8	-0.76988	-0.77209	-4.95141	-4.95143	-5.34456

^a First-order thermal quasi-particle theory or thermal HF theory.

^b Second-order thermal quasi-particle theory with zero-temperature HF reference.

^c Thermal FCI theory.¹⁸

^d Ionization energy from the corresponding MBGF.^{17,22}

TABLE VI. Thermal electron-attachment energy (in E_h) of the hydrogen fluoride molecule (0.9168 Å) in the STO-3G basis set as a function of temperature (T).

T / K	Thermal LUMO energy		$U(N + 1) - U(N)$		
	QP(1)=HF ^a	QP(2) ^b	QP(1)=HF ^a	QP(2) ^b	FCI ^c
0 ^d	0.62924	0.64424	0.62924	0.64424	0.65170
10^4	0.62924	0.64424	0.62924	0.64424	0.65170
10^5	0.48080	0.49392	0.07823	0.08932	0.40988
10^6	0.28118	0.20431	-0.55009	-0.55537	-0.12383
10^7	0.23384	0.13982	-3.14063	-3.14106	-2.71365
10^8	0.21118	0.11357	-4.90424	-4.90428	-4.48208

^a First-order thermal quasi-particle theory or thermal HF theory.

^b Second-order thermal quasi-particle theory with zero-temperature HF reference.

^c Thermal FCI theory.¹⁸

^d Electron-attachment energy from the corresponding MBGF.^{17,22}

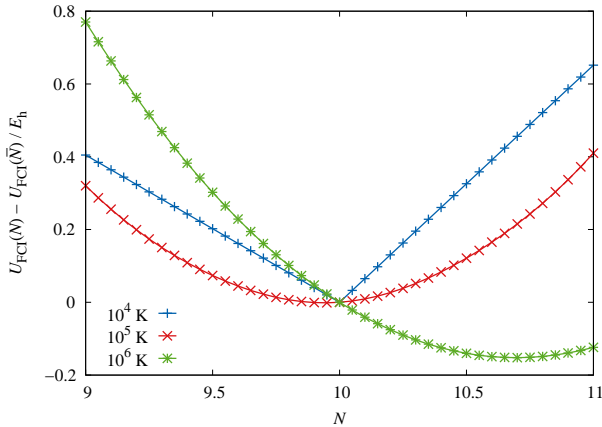


FIG. 7. Internal energy of thermal FCI theory U_{FCI} (in E_h) of the hydrogen fluoride molecule (0.9168 Å) in the STO-3G basis set as a function of the average number of electrons N relative to the value for $N = \bar{N} = 10$.

thermal FCI theory) at $T \gg 0$, notwithstanding the questionable validity of the approximation. However, $U(N) - U(N - 1)$ or $U(N + 1) - U(N)$ calculated with ϵ_p of thermal quasi-particle theories are in line with the approximate ionization or electron-attachment energies of thermal FCI theory.

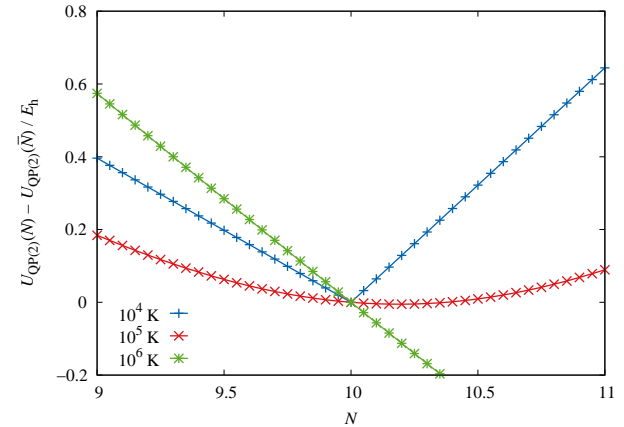


FIG. 8. Same as Fig. 7 but for the internal energy of thermal QP(2) theory $U_{\text{QP}(2)}$.

Thermal QP(2) theory is much closer to thermal FCI theory than thermal HF theory at low temperatures ($T \leq 10^4$ K), correctly accounting for electron correlation in thermal ionization and electron-attachment energies. However, at higher T , thermal HF and QP(2) theories are essentially the same, suggesting that the effect of electron correlation is surpassed

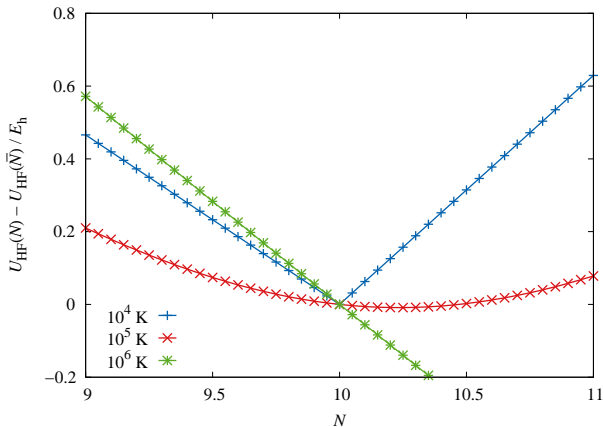


FIG. 9. Same as Fig. 7 but for the internal energy of thermal HF theory U_{HF} .

by the lack thereof in the entropy and chemical potential in the quasi-independent-particle picture.

The figures reinforce these observations, but provide the following additional insights: As T is lowered, the $U(N)$ curve begins to display the derivative discontinuity at $N = \bar{N}$, although the strict discontinuity does not occur until $T = 0$. In both the low- and high- T extremes, $U(N)$ has near-linear dependence on N within each interval between adjacent integers, but at intermediate T , $U(N)$ is a convex curve with its minimum occurring away from $N = \bar{N}$.

Let us consider the slope of $U(N)$ at $N = \bar{N}$, which is another macroscopic quantity evaluable with ϵ_p .

$$\begin{aligned} \frac{\partial U}{\partial N} &= \frac{\partial \mu}{\partial N} \sum_p \frac{\partial f_p^-}{\partial \mu} \frac{\partial U}{\partial f_p^-} \\ &= \frac{\sum_p f_p^- f_p^+ \epsilon_p}{\sum_p f_p^- f_p^+}, \end{aligned} \quad (50)$$

where we used Eq. (48) and

$$\frac{\partial f_p^-}{\partial \mu} = \beta f_p^- f_p^+. \quad (51)$$

This is the increase in the internal energy upon infusion of an infinitesimal fraction of an electron into every molecule in the ideal gas. It is a weighted average of ϵ_p over all spinorbitals with the p th spinorbital weight being $f_p^- f_p^+$. It corresponds neither to the ionization nor to the electron-attachment process because it is oblivious to the sign of the variation in N . However, in the $T = 0$ limit, it distinguishes these two processes by exhibiting the derivative discontinuity, i.e.,

$$\lim_{T \rightarrow 0} \left(\frac{\partial U}{\partial N} \right)_{N=\bar{N}^-} = \epsilon_{\text{HOMO}}, \quad (52)$$

$$\lim_{T \rightarrow 0} \left(\frac{\partial U}{\partial N} \right)_{N=\bar{N}^+} = \epsilon_{\text{LUMO}}. \quad (53)$$

Until the $T = 0$ limit is strictly reached, however, the $U(N)$ curve is smooth everywhere and the slope approaches the mid-

TABLE VII. $\partial U / \partial N$ ((in E_h)) of the hydrogen fluoride molecule (0.9168 Å) in the STO-3G basis set as a function of temperature (T).

T / K	QP(1)=HF ^a	QP(2) ^b	FCI ^c
0 ^d	0.08253	0.12433	0.12371
10^4	0.08189	0.12461	0.12351
10^5	-0.07423	-0.05604	0.04959
10^6	-0.56092	-0.56475	-0.44097
10^7	-3.26523	-3.26554	-3.17327
10^8	-4.92771	-4.92775	-4.91206

^a First-order thermal quasi-particle theory or thermal HF theory [Eq. (50)].

^b Second-order thermal quasi-particle theory with zero-temperature HF reference [Eq. (50)].

^c Thermal FCI theory (numerical differentiation).¹⁸

^d The average of ionization and electron-attachment energies of the corresponding MBGF.^{17,22}

point of the HOMO and LUMO energies. For $T \approx 0$,

$$\left(\frac{\partial U}{\partial N} \right)_{N=\bar{N}} \approx \frac{\epsilon_{\text{HOMO}} + \epsilon_{\text{LUMO}}}{2}, \quad (54)$$

which is also equal to the $T = 0$ limit of the μ .^{10,27}

Table VII compares the slope $\partial U / \partial N$ at $N = \bar{N}$ computed analytically by Eq. (50) for thermal HF and QP(2) theories against the slope of thermal FCI theory obtained by numerical differentiation. The three sets of values are in reasonable agreement with one another at all T considered. At low T , thermal QP(2) theory is in much better agreement with thermal FCI theory than thermal HF theory as the former takes into account electron correlation. At higher T , thermal QP(2) and HF theories are more alike than thermal FCI theory, but they all seem to converge at the same high T limit.

To summarize the results of the foregoing analysis, the orbital energies ϵ_p of thermal quasi-particle theories (including thermal HF theory) cannot be directly related to the ionization or electron-attachment energy from/into the p th orbital except at $T = 0$. This is simply because an ionization in an ideal gas of molecules at $T \gg 0$ is not a removal of an electron from the p th orbital in every molecule; rather, it is a removal of an electron from various orbitals of all molecules at some probabilities (even in a strict independent-particle picture). This is, in turn, equivalent to a removal of some fraction of an electron from various orbitals of a single average molecule. The ϵ_p at $T > 0$ signifies the increase in internal energy upon adding an infinitesimal fraction of an electron in the p th spinorbital of this “average” molecule. This quantity may not directly correspond to any observable, but it can be combined to produce a macroscopic thermodynamic observable, for which thermal QP(2) theory is in better agreement with thermal FCI theory than thermal HF theory.

VII. CONCLUSIONS

The thermal quasi-particle theory has been introduced. It is a quasi-independent-particle theory and a finite-temperature extension of the widely used thermal HF theory. Its entropy

and chemical-potential formulas are of the one-electron type,

$$S \equiv -k_B \sum_p (f_p^- \ln f_p^- + f_p^+ \ln f_p^+),$$

and

$$\bar{N} \equiv \sum_p f_p^-$$

where the thermal population f_p^- is also unchanged from the Fermi-Dirac distribution function,

$$f_p^- \equiv \frac{1}{1 + e^{\beta(\epsilon_p - \mu)}},$$

and $f_p^+ = 1 - f_p^-$. The orbital energies ϵ_p now become the ones that include the effect of electron correlation by being defined as the correlated, thermal one-electron energies in the spirit of MBGF,

$$\epsilon_p \equiv \frac{\partial U}{\partial f_p},$$

where U is a correlated internal energy, whose mathematical form can be postulated on the basis of finite-temperature MBPT through any chosen order. When the grand potential is defined by

$$\Omega \equiv U - \mu \bar{N} - TS,$$

the theory satisfies all thermodynamic relations and the Ω is a variational minimum with respect to f_p^- .

Fermi-Dirac and thermal HF theories can be viewed as the zeroth- and first-order instances, respectively, in the hierarchy of thermal quasi-particle theories. It can be viewed as a diagonal, frequency-independent approximation to a finite-temperature extension of the inverse Dyson equation, which is an exact one-particle theory.¹⁷ In other words, the ϵ_p thus defined is a finite-temperature extension of the Dyson self-energy in the diagonal, frequency-independent approximation. Generally, the thermal self-energy is shown to suffer from the severe kind of Kohn-Luttinger nonconvergence problem and so it is inappropriate to include anomalous-diagram terms in the definition of approximate U or Ω .

Our preliminary implementation and comparison with the thermal FCI benchmarks suggests that thermal QP(2) theory performs distinctly better than thermal HF theory at low T and may even outperform finite-temperature MBPT(2) at intermediate T by including electron-correlation effects in the orbital energies. At higher T , the entropy contribution dominates and the differences among various methods become relatively insignificant.

The direct physical meaning of ϵ_p is the increase in internal energy upon infusion of an infinitesimal fraction of an electron in the p th spinorbital. It does not correspond to the ionization energy or electron-attachment energy of a molecule at $T > 0$. However, it can be used as ingredients from which electron-correlated thermodynamic observables can be computed.

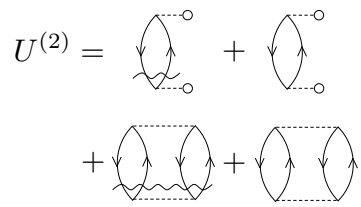


FIG. 10. Second-order internal energy diagrams of Eq. (A3), which include anomalous (second and fourth) diagrams with no resolvent lines.

ACKNOWLEDGMENTS

This work was supported by the U.S. Department of Energy (DoE), Office of Science, Office of Basic Energy Sciences under Grant No. DE-SC0006028 and also by the Center for Scalable Predictive methods for Excitations and Correlated phenomena (SPEC), which is funded by the U.S. DoE, Office of Science, Office of Basic Energy Sciences, Division of Chemical Sciences, Geosciences and Biosciences as part of the Computational Chemical Sciences (CCS) program at Pacific Northwest National Laboratory (PNNL) under FWP 70942. PNNL is a multi-program national laboratory operated by Battelle Memorial Institute for the U.S. DoE. The author is a Guggenheim Fellow of the John Simon Guggenheim Memorial Foundation.

Appendix A: Kohn-Luttinger nonconvergence

According to finite-temperature MBPT,¹⁰⁻¹² a more complete expression for the second-order internal energy should include the so-called anomalous-diagram contributions.²⁶ It may read

$$U^{\text{QP}} \equiv \langle E^{(0)} \rangle + \langle E^{(1)} \rangle + U^{(2)} \quad (\text{A1})$$

with

$$\begin{aligned} U^{(2)} &\equiv \langle E^{(2)} \rangle - \beta \langle E^{(1)} E^{(1)} \rangle + \beta \langle E^{(1)} \rangle \langle E^{(1)} \rangle \\ &= \langle E^{(2)} \rangle - \beta \langle E^{(1)} E^{(1)} \rangle_L, \end{aligned} \quad (\text{A2})$$

where subscript “ L ” means that only diagrammatically linked contributions are to be retained, and the last term (carrying a β multiplier) is the anomalous-diagram term. This is still far from the whole second-order internal energy [Eq. (74) of Ref. 11], but the presence of the last anomalous-diagram term will make the following analysis meaningful.

The zeroth-order thermal averages in the above expression

can be evaluated^{11,12} as

$$\begin{aligned}
U^{(2)} = & \sum_{p,q}^{\text{denom.}\neq 0} \frac{F_{qp}F_{pq}}{\epsilon_p^{(0)} - \epsilon_q^{(0)}} f_p^- f_q^+ \\
& - \beta \sum_{p,q}^{\text{denom.}=0} F_{qp}F_{pq} f_p^- f_q^+ \\
& + \frac{1}{4} \sum_{p,q,r,s}^{\text{denom.}\neq 0} \frac{\langle pq||rs\rangle\langle rs||pq\rangle}{\epsilon_p^{(0)} + \epsilon_q^{(0)} - \epsilon_r^{(0)} - \epsilon_s^{(0)}} f_p^- f_q^- f_r^+ f_s^+ \\
& - \frac{\beta}{4} \sum_{p,q,r,s}^{\text{denom.}=0} \langle pq||rs\rangle\langle rs||pq\rangle f_p^- f_q^- f_r^+ f_s^+, \quad (\text{A3})
\end{aligned}$$

whose diagrammatic representation is given in Fig. 10.

The second and fourth terms (carrying a β multiplier but no denominator) are anomalous-diagram terms,²⁶ causing the low-temperature breakdown known as the Kohn–Luttinger nonconvergence.^{14,26–28} Take the second term for example. The “denom.=0” restricts the summation to over those combinations of indexes whose fictitious denominator $\epsilon_p^{(0)} - \epsilon_q^{(0)}$ is zero. One such combination is $p = q$. As T is lowered to zero (i.e., $\beta \rightarrow \infty$),²⁶

$$\lim_{T \rightarrow 0} \beta f_p^- f_p^+ = \delta(\mu - \epsilon_p^{(0)}), \quad (\text{A4})$$

where the right-hand side is Dirac’s δ function, which is divergent when the chemical potential μ coincides with one of the orbital energies.²⁶ Therefore, a Kohn–Luttinger nonconvergence occurs when $F_{pp} \neq 0$ and at the same time, the reference wave function is degenerate (i.e., the HOMO and LUMO have the same energy as μ). While the divergence of this term can still be avoided by adopting a HF reference wherein $F_{pq} = 0$,¹⁴ the fourth term remains divergent for $p = r$ and $q = s$ in a degenerate reference.^{27,28} It should be recalled that the second-order correction to the ground-state energy is always finite regardless of whether the zeroth-order ground state is degenerate¹⁹ or nondegenerate.⁷ Hence, $U^{(2)}$ is not convergent at the correct zero-temperature limit, which is always finite.

As per Eq. (42), the corresponding thermal self-energy is obtained by taking the derivative of $U^{(2)}$ with respect to f_p^- ,

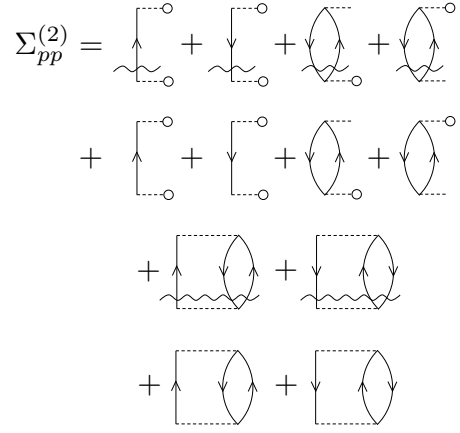


FIG. 11. Second-order thermal Dyson self-energy diagrams of Eq. (A5), which include anomalous diagrams with no resolvent lines. They are obtained by cutting an edge in each of the internal energy diagrams of Fig. 10 and trimming the dangling lines.

i.e.,

$$\begin{aligned}
\Sigma_{pp}^{(2)} & \equiv \frac{\partial U^{(2)}}{\partial f_p^-} \\
& = \sum_q^{\text{denom.}\neq 0} \frac{F_{qp}F_{pq}}{\epsilon_p^{(0)} - \epsilon_q^{(0)}} f_q^+ - \sum_q^{\text{denom.}\neq 0} \frac{F_{qp}F_{pq}}{\epsilon_q^{(0)} - \epsilon_p^{(0)}} f_q^- \\
& + \sum_{q,r}^{\text{denom.}\neq 0} \frac{\langle qr||pr\rangle F_{pq}}{\epsilon_p^{(0)} - \epsilon_q^{(0)}} f_p^- f_q^+ \\
& + \sum_{q,r}^{\text{denom.}\neq 0} \frac{F_{qp}\langle pr||qr\rangle}{\epsilon_p^{(0)} - \epsilon_q^{(0)}} f_p^- f_q^+ \\
& - \beta \sum_q^{\text{denom.}=0} F_{qp}F_{pq} f_q^+ + \beta \sum_q^{\text{denom.}=0} F_{qp}F_{pq} f_q^- \\
& - \beta \sum_{q,r}^{\text{denom.}=0} \langle qr||pr\rangle F_{pq} f_p^- f_q^+ \\
& - \beta \sum_{q,r}^{\text{denom.}=0} F_{qp}\langle pr||qr\rangle f_p^- f_q^+ \\
& + \frac{1}{2} \sum_{q,r,s}^{\text{denom.}\neq 0} \frac{\langle pq||rs\rangle\langle rs||pq\rangle}{\epsilon_p^{(0)} + \epsilon_q^{(0)} - \epsilon_r^{(0)} - \epsilon_s^{(0)}} f_q^- f_r^+ f_s^+ \\
& - \frac{1}{2} \sum_{q,r,s}^{\text{denom.}\neq 0} \frac{\langle rs||pq\rangle\langle pq||rs\rangle}{\epsilon_r^{(0)} + \epsilon_s^{(0)} - \epsilon_p^{(0)} - \epsilon_q^{(0)}} f_q^+ f_r^- f_s^- \\
& - \frac{\beta}{2} \sum_{q,r,s}^{\text{denom.}=0} \langle pq||rs\rangle\langle rs||pq\rangle f_q^- f_r^+ f_s^+ \\
& + \frac{\beta}{2} \sum_{q,r,s}^{\text{denom.}=0} \langle rs||pq\rangle\langle pq||rs\rangle f_q^+ f_r^- f_s^-. \quad (\text{A5})
\end{aligned}$$

The corresponding diagrams are shown in Fig. 11, which are obtained by opening each of the $U^{(2)}$ diagrams in Fig. 10 by deleting an edge.

This formula suffers from a more pervasive kind of the Kohn–Luttinger nonconvergence problem. Take the penultimate term for example. It sums over the $p = r$ and $q = s$ case, whose summand diverges as $T \rightarrow 0$ ($\beta \rightarrow \infty$) for any reference—degenerate or nondegenerate—because a f_p^- factor is no longer there to create a δ function [Eq. (A4)] which diverges only when $\mu = \epsilon_p^{(0)}$. In other words, a finite-temperature generalization of the self-energy, when it is derived more rigorously from finite-temperature MBPT and thus includes anomalous-diagram terms, is far more prone to divergence as $T \rightarrow 0$ and will be uselessly erroneous at low T . This is not surprising because in thermodynamics all states with any number of electrons are summed over in the partition function and they always include numerous exactly degenerate zeroth-order states.

This finding may bode ill for the Luttinger–Ward functional^{14,29,30,44–48} because opening a diagram of this functional will result in a thermal self-energy or Green’s function diagram that may always suffer from the same severe low-temperature breakdown.

Appendix B: Feynman–Dyson nonconvergence

In Ref. 22 was reported that a Feynman–Dyson perturbation expansion of the Dyson self-energy is always divergent

in many frequency domains. Therefore, even apart from the divergence of the *thermal* self-energy caused by anomalous-diagram terms analyzed in Appendix A, the *zero-temperature* self-energy is expected to be divergent or at least excessively erroneous for low- and high-lying states. This is alleviated (or hidden from view) by the frequency-independent approximation inherent in the ansatz of thermal quasi-particle theory, but in a solid, whose self-energy forms continuous energy bands, we can no longer expect to be able to avoid this deep-rooted pathology.²²

We therefore expect that in a solid-state implementation of thermal QP(2) theory (which is underway in our laboratory), we will introduce active orbitals (or active energy bands) and define and evaluate portions of $\langle E^{(2)} \rangle$ and of $\Sigma_{pp}^{(2)}$ involving these orbitals. These active orbitals are the ones whose zeroth-order energies fall within the so-called “central overlapping bracket” where the Feynman–Dyson perturbation expansion is guaranteed to have a nonzero radius of convergence.²² Comparative performance of this method for solids will be presented in the future.

* sohirata@illinois.edu

¹ K. Husimi, Proc. Phys. Math. Soc. Jpn. **22**, 264 (1940).

² N. D. Mermin, Ann. Phys. **21**, 99 (1963).

³ P. Gu and S. Hirata, Journal **Vol.**, page (the preceding article) (2024).

⁴ B. Farid, N. H. March, and A. K. Theophilou, Phys. Rev. E **62**, 134 (2000).

⁵ P. N. Argyres, T. A. Kaplan, and N. P. Silva, Phys. Rev. A **9**, 1716 (1974).

⁶ A. Szabo and N. S. Ostlund, *Modern Quantum Chemistry* (MacMillan, New York, 1982).

⁷ I. Shavitt and R. J. Bartlett, *Many-Body Methods in Chemistry and Physics* (Cambridge University Press, Cambridge, 2009).

⁸ M. R. Hermes and S. Hirata, J. Chem. Phys. **143**, 102818 (2015).

⁹ J. C. Pain, J. Phys. B. At. Mol. Opt. **44**, 145001 (2011).

¹⁰ S. Hirata and P. K. Jha, Annu. Rep. Comput. Chem. **15**, 17 (2019).

¹¹ S. Hirata and P. K. Jha, J. Chem. Phys. **153**, 014103 (2020).

¹² S. Hirata, J. Chem. Phys. **155**, 094106 (2021).

¹³ T. Matsubara, Prog. Theor. Phys. **14**, 351 (1955).

¹⁴ J. M. Luttinger and J. C. Ward, Phys. Rev. **118**, 1417 (1960).

¹⁵ N. H. March, W. H. Young, and S. Sampath, *The Many-Body Problem in Quantum Mechanics* (Cambridge University Press, Cambridge, 1967).

¹⁶ L. P. Kadanoff and G. Baym, *Quantum Statistical Mechanics* (CRC Press, Boca Raton, 2018).

¹⁷ S. Hirata, A. E. Doran, P. J. Knowles, and J. V. Ortiz, J. Chem. Phys. **147**, 044108 (2017).

¹⁸ Z. Kou and S. Hirata, Theor. Chem. Acc. **133**, 1487 (2014).

¹⁹ J. O. Hirschfelder and P. R. Certain, J. Chem. Phys. **60**, 1118 (1974).

²⁰ R. J. Bartlett, Annu. Rev. Phys. Chem. **32**, 359 (1981).

²¹ S. Hirata, M. R. Hermes, J. Simons, and J. V. Ortiz, J. Chem. Theory Comput. **11**, 1595 (2015).

²² S. Hirata, I. Grabowski, J. V. Ortiz, and R. J. Bartlett, Phys. Rev. A **109**, 052220 (2024).

²³ G. D. Purvis and Y. Öhrn, Chem. Phys. Lett. **33**, 396 (1975).

²⁴ J. Schirmer and G. Angonoa, J. Chem. Phys. **91**, 1754 (1989).

²⁵ J. V. Ortiz, J. Chem. Phys. **153**, 070902 (2020).

²⁶ W. Kohn and J. M. Luttinger, Phys. Rev. **118**, 41 (1960).

²⁷ S. Hirata, Phys. Rev. A **103**, 012223 (2021).

²⁸ S. Hirata, Chem. Phys. Lett. **800**, 139668 (2022).

²⁹ G. Baym and L. P. Kadanoff, Phys. Rev. **124**, 287 (1961).

³⁰ G. Baym, Phys. Rev. **127**, 1391 (1962).

³¹ D. Van Neck, M. Waroquier, and J. Ryckebusch, Nucl. Phys. A **530**, 347 (1991).

³² W. H. Dickhoff, “The nucleon propagator in the nuclear medium,” in *Nuclear Methods and the Nuclear Equation of State*, International Review of Nuclear Physics, Vol. 8, edited by M. Baldo (World Scientific, Singapore, 1999) Chap. 7, pp. 326–380.

³³ W. H. Dickhoff and C. Barbieri, Prog. Part. Nucl. Phys. **52**, 377 (2004).

³⁴ N. E. Dahlen and R. van Leeuwen, J. Chem. Phys. **122**, 164102 (2005).

³⁵ C. Barbieri, Phys. Lett. B **643**, 268 (2006).

³⁶ C. Barbieri and W. H. Dickhoff, Int. J. Mod. Phys. A **24**, 2060 (2009).

³⁷ J. J. Phillips and D. Zgid, J. Chem. Phys. **140**, 241101 (2014).

³⁸ D. Neuhauser, R. Baer, and D. Zgid, J. Chem. Theory Comput. **13**, 5396 (2017).

³⁹ W. Tarantino, P. Romaniello, J. A. Berger, and L. Reining, Phys. Rev. B **96**, 045124 (2017).

⁴⁰ C. J. N. Coveney and D. P. Tew, J. Chem. Theory Comput. **19**,

3915 (2023).

⁴¹ M. E. Fisher and D. Ruelle, *J. Math. Phys.* **7**, 260 (1966).

⁴² F. J. Dyson and A. Lenard, *J. Math. Phys.* **8**, 423 (1967).

⁴³ S. Hirata and Y. Ohnishi, *Phys. Chem. Chem. Phys.* **14**, 7800 (2012).

⁴⁴ E. Kozik, M. Ferrero, and A. Georges, *Phys. Rev. Lett.* **114**, 156402 (2015).

⁴⁵ R. Rossi and F. Werner, *J. Phys. A* **48**, 485202 (2015).

⁴⁶ A. R. Welden, A. A. Rusakov, and D. Zgid, *J. Chem. Phys.* **145**, 204106 (2016).

⁴⁷ O. Gunnarsson, G. Rohringer, T. Schäfer, G. Sangiovanni, and A. Toschi, *Phys. Rev. Lett.* **119**, 056402 (2017).

⁴⁸ L. Lin and M. Lindsey, *Proc. Natl. Acad. Sci. (USA)* **115**, 2282 (2018).